taxonomy

MDPI

Article

Comparison of Seed Images with Geometric Models, an Approach to the Morphology of *Silene* (Caryophyllaceae)

José Javier Martín-Gómez [1], José Luis Rodríguez-Lorenzo [2], Bohuslav Janoušek [2], Ana Juan [3] and Emilio Cervantes [1,*]

[1] IRNASA-CSIC, Cordel de Merinas, 40, 37008 Salamanca, Spain
[2] Plant Developmental Genetics, Institute of Biophysics v.v.i, Academy of Sciences of the Czech Republic, Královopolská 135, 612 65 Brno, Czech Republic
[3] Departamento de Ciencias Ambientales y Recursos Naturales, University of de Alicante, San Vicente del Raspeig, 03690 Alicante, Spain
* Correspondence: emilio.cervantes@irnasa.csic.es; Tel.: +34-923219606

Abstract: Seed morphological description is traditionally based on adjectives, which originated from the comparison with other shapes, including geometric figures. Nevertheless, descriptions based on this feature are not quantitative and measurements giving the percentage of similarity of seeds with reference figures are not available in the literature. Lateral views of *Silene* seeds resemble the cardioid and cardioid-derived figures. Dorsal views, nonetheless, resemble ellipses and derivatives, allowing seed shape quantification by comparison with defined geometric figures. In this work, we apply already-described models as well as new models to the morphological analysis of 51 *Silene* species. Our data revealed the existence of a link between lateral and dorsal models. Lateral models closed in the hilum region (models LM2 and LM4) were associated with those convex models of the dorsal seed views (DM1-DM4, DM10). Lateral models more open around the hilum region adjusted to seeds characterized as *dorso canaliculata* type better, i.e., to those geometric models with partial concavities in their dorsal views. The relationship between lateral and dorsal models, as well as between the models to their utility in taxonomy, is discussed.

Keywords: cardioid; ellipse; geometry; seeds; silhouettes; taxonomy

Citation: Martín-Gómez, J.J.; Rodríguez-Lorenzo, J.L.; Janoušek, B.; Juan, A.; Cervantes, E. Comparison of Seed Images with Geometric Models, an Approach to the Morphology of *Silene* (Caryophyllaceae). *Taxonomy* **2023**, *3*, 109–132. https://doi.org/10.3390/taxonomy3010010

Academic Editor: Tod Stuessy

Received: 21 December 2022
Revised: 2 February 2023
Accepted: 6 February 2023
Published: 9 February 2023

1. Introduction

Seed shape diversity observed in *Silene* has long been recognized as a valuable source of information for infrageneric classification. Seed morphological characters have been used with diverse applications in the taxonomy of this genus [1–11]. In relation to general seed shape, the description is traditionally based on adjectives such as *reniformia* [1,2], reniform, reniform-circular [3–8]; half-rounded, flabellate [7]; round-reniform, symmetrical-reniform, cordate-reniform, asymmetrical-reniform, semicircle-reniform [8]; and ovate or winged [9]. Recently, a relationship between the surface structure and the overall outline seed morphology has been described [12,13]. Based on the seed surface outline of 52 species of *Silene* and two closely related genera (*Atocion* and *Viscaria*), a classification in four groups was proposed (smooth, rugose, echinate, and papillose) [13]. This seed classification showed a certain association with the taxonomic treatment of the currently defined subgenera. Hence, the group of smooth seeds was mostly composed of species of *S.* subg. *Silene* while the majority of the echinate seeds corresponded to a species of *S.* subg. *Behenantha*.

As a new morphological approach, we have described the lateral and dorsal views of *Silene* seeds comparing the seed contour with algebraically defined geometric figures, such as the cardioid, modified cardioid, or diverse ellipses. We provided a *J* index, a numerical value indicating the percentage of similarity between a defined seed silhouette and a given geometric figure, taken as a model [14–18]. The comparison of lateral seed

views in geometric models was applied for the first time in *Silene* for 21 species with the basic model LM1 (the cardioid) and the values of the *J* index were over 90 in 11 species of *Silene* subg. *Behenantha* (*S. acutifolia* Link ex Rohrb., *S. conica* L., *S. diclinis* (Lag.) M.Laínz, *S. dioica* (L.) Clairv., *S. latifolia* Poir., *S. noctiflora* L., *S. pendula* L., *S. uniflora* Roth, *S. viscosa* (L.) Pers., *S. vulgaris* (Moench) Garcke and *S. zawadskii* Herbich), and 7 species of *S.* subg. *Silene* (*S. gallica* L., *S. italica* (L.) Pers., *S. nutans* L., *S. otites* (L.) Wibel, *S. portensis* L., *S. saxifraga* L., and *S. vivianii* Steud.) [14]. Nevertheless, seeds of *S. diclinis* and *S. latifolia* had higher *J* index values in the additional models LM2 and LM4 (derived from the cardioid, LM1), than in the cardioid model. Seeds of *S. gallica* had the highest value in another geometric model LM3 [14].

The research continued with the description of new models for the lateral view (LM5 to LM8) based on the analysis of 20 *Silene* species. From these 20 species, 16 (*S. coutinhoi* Rothm. and P.Silva, *S. crassipes* Fenzl., *S. disticha* Willd., *S. diversifolia* Otth., *S. foetida* Link ex Spreng., *S. littorea* Brot., *S. micropetala* Lag., *S. muscipula* L., *S. nicaeensis* All., *S. nocturna* L., *S. portensis* L., *S. scabriflora* Brot., *S. sclerocarpa* Dufour, *S. stricta* L., *S. tridentata* Desf., and *S. vivianii*) were analyzed for the first time, extending the analysis to a total of 37 *Silene* species [15]. This work revealed the potential existence of four defined seed groups according to the aspect ratio in their dorsal views. The new geometric models gave the best results with *S. diversifolia* and *S. tridentata* (LM5), *S. coutinhoi* (LM7) and *S. nicaeensis*, *S. portensis*, and *S. scabriflora* (LM8). In addition, a preliminary correspondence was found between lateral models and the convexity values in the dorsal views. Those convex seeds in their dorsal views adjusted well to models LM2 and LM4, while seeds that presented concavities in their dorsal views adjusted better to other lateral models (LM3, LM5, and LM6).

A new approach was recently conducted based on dorsal views and the relationship between their morphology and the geometric models. Rodríguez-Lorenzo et al. [16] reported new models for dorsal views of seeds, together with new data from the *J* index for the lateral views of the species *S. inaperta* L., *S. pseudoatocion* Desf., and *S. ramosissima* Desf. in the lateral geometric model LM1. Dorsal seed views adjusted to nine models (DM1–DM9), which corresponded to convex (DM1–DM4) and non-convex (DM5–DM9) model types. The species related to convex models were *S. diclinis*, *S. dioica*, *S. foetida*, *S. latifolia*, and *S. vulgaris*; those with non-convex models were *S. conica*, *S. coutinhoi*, *S. inaperta*, and *S. ramosissima*.

Based on the data set out above, the description and quantification of seed shape with geometric models revealed a certain level of differentiation among species, and this morphological tool constitutes a promising technique for the taxonomy of species, especially for *Silene*. An example of the description and taxonomical use of lateral and dorsal models was reported by Martin-Gómez et al. [17] for the *S. mollissima* (L). Pers. aggregate. The images of seeds of this group of species adjusted to three lateral (LM1, LM4, and LM5) and two dorsal models (DM5 and DM6) [17]. The authors reported that the degree of similarity of the seeds to the model LM5 revealed the identification of two groups of species with different geographic origin. This work highlighted the stability of seed shape measured by comparison with a geometric models in contrast to other common morphological measurements (e.g., seed size).

The objectives of the present work were (i) to apply a seed description based on geometric models to non-previously analyzed *Silene* species, (ii) to identify the differences between these species, and (iii) to establish a correspondence between the groups based on their surface and geometric models describing the overall shape in the lateral and dorsal views of these *Silene* species. We hypothesize that the obtained information may provide new useful knowledge to understand the relationships among species as well as providing new comparative information for their characterization and classification using this morphological approach.

2. Materials and Methods

2.1. Seeds

The seeds used in this work are described in Table A1 (see Appendix A). They belong to populations of 51 *Silene* species and the species *Eudianthe coeli-rosa*, which proceed from laboratories and botanical gardens through a program of international cooperation with the seed collection (Carpoespermateca) of the botanical garden at the University of Valencia. They were sent to IRNASA-CSIC in June 2022. The seed images used in the analysis are stored in Zenodo (see Supplementary Materials) and a description of their silhouettes has been given [13].

The plant nomenclature (genera, subgenera, sections, species, and subspecies) and the taxa authorities were adapted according to Plants of the World Online (POWO) [19]. The taxonomical classification in subgenera and sections of the genus *Silene* follows Jaffari et al. [20].

2.2. Photography

Lateral and dorsal views of these seeds used in the morphological analysis were taken with a Nikon Z6 camera equipped with an objective AF-S Micro NIKKOR 60 mm f/2.8G ED.

2.3. Image Preparation

Twenty seeds per species were selected both for the lateral and dorsal views and ordered (aligned) in a document (.PSD format of Corel Photo Paint). This document containing the aligned seeds was used to obtain average silhouettes for the lateral and dorsal views of the seeds using the method described [15,21]. A video describing the method used is available (see Supplementary Materials).

The average silhouettes for the lateral and dorsal views (L and D, respectively) of each species were assembled in image archives (.PSD). The white and black images of models were superimposed to the average silhouettes for each species in the assembled .PSD images, and the *J* index was calculated (see below 2.5).

2.4. Models

Some of the lateral and dorsal models used here were previously described in [14,16], as shown in Figure 1 (LM1 to LM8) and Figure 2 (DM1 to DM9). In addition, 4 new dorsal models were obtained for this work based on Fourier transform [18], to get the best adjustments between the seed contour and the *J* index values (see results section).

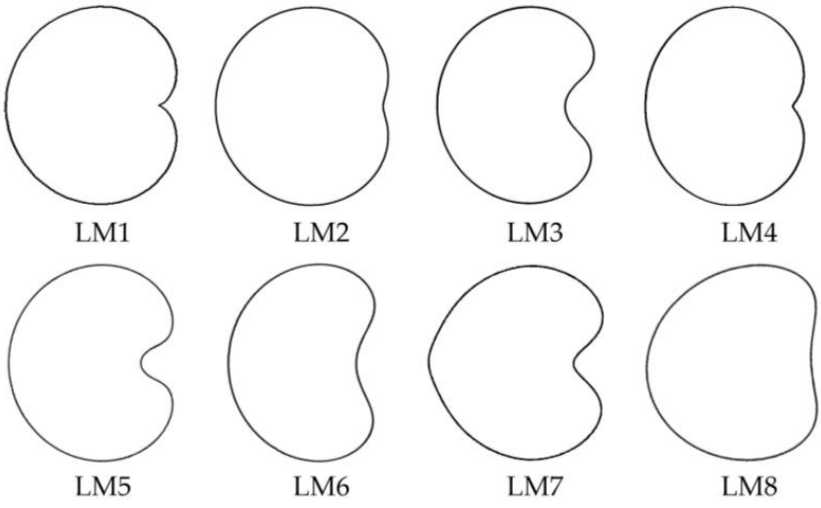

Figure 1. Lateral models (LM) used in this work, taken from [14].

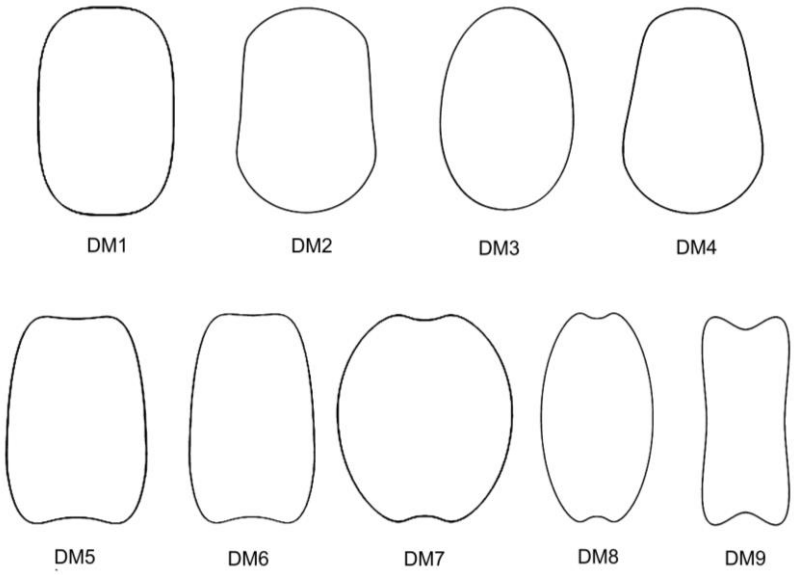

Figure 2. Dorsal models (DM) used in this work, taken from [16].

2.5. Development of New Models

New models DM10 to DM13 were obtained by elliptic Fourier transform as described [18]. Basically, a set of points (between 60 and 100) were taken from the average silhouettes of seeds for a given species or combination of species (average silhouette of average silhouettes), and the resulting Fourier curves were used as models. Models DM11, DM12, and DM13 were specifically designed for *S. chlorantha* (Willd.) Ehrh, *S. linicola* C.C. Gmel., and *S. damascena* Boiss. and Gaill, respectively (see the corresponding average silhouettes in Figure A1 of Appendix A), while DM10 was designed for the seeds of the species *S. aprica* Turcz. ex Fisch. and C.A. Mey, *S. chungtienensis* (Speg.) Bocquet, *S. dichotoma* Ehrh., *S. multiflora* (Erhr.) Pers, and *S. viridiflora* L. The Mathematica code for these models has been stored in Zenodo (see Supplementary Materials). More details about these models are given in the results section.

2.6. Similarity of the Seed Silhouettes with Models (J Index Calculation)

The similarity of the seed images with models was evaluated as the *J* index. The *J* index was calculated both for the average silhouette and for the mean of 20 seeds representative of each species, as:

$$J = S/T \times 100 \quad (1)$$

where *S* is the area shared between the seed and the model, and *T* is the total area occupied by both images. The *J* index has a maximum value of 100, corresponding to the cases where the geometric model and the seed image areas coincide. The adjustments are considered good when *J* index values are superior to 90. The value of *S* (shared area) is obtained in Image J by the superposition of the seed silhouette with a model in white, and the value of *T* (total area) is obtained by the superposition of the seed silhouette with a model in black. Representative images with the models in white and in black superimposed to the silhouettes are shown in Figure 3.

The *J* index was calculated on the average silhouettes for the lateral and dorsal views first, in each species with models LM1 to LM8 and DM1 to DM9 (excluded DM7 because of low similarity), respectively. The results obtained with the average silhouettes give an orientation at which models best adjust to the seeds, so the analysis involving mean values of 20 seeds is undertaken only in the models that give higher scores on the average silhouettes. The results obtained in LM1 (the cardioid) were excluded because it is less discriminant than the other lateral models.

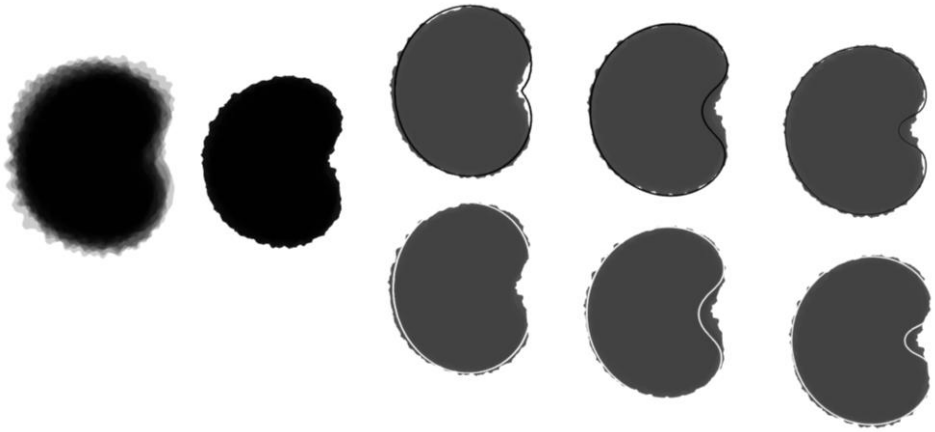

Figure 3. Method to obtain the *J* index in the average silhouette of *Eudianthe coeli-rosa*. From left to right: superimposed silhouettes of 20 seeds (lateral views); average silhouette; in 2 descending rows, left to right, average silhouette with models superimposed: LM4, LM3, and LM5, in black (above) and white (below). Area quantification with Image J in the compositions above (with the models in black) gives total area (T), while quantification in the compositions below (with the models in white) gives the values of the area shared by the average silhouette and the model (S). The *J* index is the ratio S/Tx100. The method is identical for individual seeds excluding the first step (obtention of the average silhouette).

2.7. Statistical Analysis

The Euclidean distance and Ward algorithm for clustering were used to calculate the dendrogram. The matrix used for the analysis combined the data for LM2/4 and LM5 (Table A7 in Appendix A). The ten best scores obtained with each model in the species were used. Statistical analysis was done with IBM SPSS statistics SPSS es 29.0.0.0 (241).

3. Results

3.1. Average Seed Silhouettes

Figure A1 (Appendix A) shows the average silhouettes for the lateral and dorsal views of seeds of 51 *Silene* species and *Eudianthe coeli-rosa*. The average silhouettes of the seeds reveal important aspects of their morphology, such as general symmetry, aspect ratio (equal to ratio length/width), and convexity for both the lateral and dorsal seed views. Average silhouettes in the dorsal views for the majority of seeds are convex. Nevertheless, concavities in the upper and lower seed views are notable in some species (e.g., *S. damascena*, *S. frivaldskyana*, *S. roemeri*, *S. ruprechtii*, or *S. saxatilis*), most of them belonging to S. subg. *Silene*. A detailed study of the morphological measurements and the geometry of these seeds was already presented [13].

3.2. J Index Calculations on Average Silhouettes

3.2.1. Lateral Models

The results of *J* index calculations on average silhouettes for 51 *Silene* species were grouped into two tables, separating those species giving maximum values of *J* index in models LM2, LM4, and LM8 (Table A2 in Appendix A, with 43 species), from those giving maximum *J* index values in model LM5 (Table A3, with 8 species). Models LM6 and LM7 did not give maximum values in any species. The seeds of species associated with model LM5 (Table A3) are characterized by more open lateral views with larger concavities in the hilum zone, while those resembling models LM2, LM4, and LM8 (Table A2) are more closed, tending to be convex (higher solidity values [12]). From the 43 species in Table A2, 19 belong to S. subg. *Behenantha*, and 24 to S. subg. *Silene*. All species in Table A3 from model LM5 belong to S. subg. *Silene*.

3.2.2. Dorsal Models

The results were grouped into three tables, corresponding, respectively, to convex models DM1 to DM4 (Table A4), intermediate models with low degrees of concavity (models DM5 and DM6; Table A5), and models with notable concavities in the poles (DM8 and DM9; Table A6). Model DM7 did not give good results with any of the species tested in this work. Maximum values of *J* index with models DM1 to DM4 were obtained in 10 species (Table A4), all of them included in Table A2 of species with similarity to models LM2 and LM4. Out of the nine species in Table A4, six species (66.6%) belong to *Silene* subg. *Behenantha*. Maximum values in models DM5 and/or DM6 were obtained in 23 species, of which eight (34.8%) belong to *Silene* subg. *Behenantha*. A total of 17 species gave maximum values in other models (DM7 and DM8; Table A6). Of these, five belong to *Silene* subg. *Behenantha* (31.6%), four corresponded to *Silene* sect. *Physolychnis*, and one to *Silene* sect. *Cucubaloides* (*S. yunnanensis*). In general, the average silhouettes of seeds in Table A6 are more elongated in their dorsal views (higher aspect ratio).

3.3. New Models for the Dorsal Views of Silene Species

The new models are shown in Figure 4. DM10 corresponds to a hyperellipse and it is a convex figure. It differs from DM1 in a certain asymmetry between the terminal sides, since the lower one is slightly broader than the upper side (Figures 1 and 4). The model DM11 also resembles DM1, but it is narrower and has small concave regions in the four sides (Figures 1 and 4). DM12 and 13 are figures with partial concavity regions for the upper and lower sides (Figure 4), designed for *S. linicola* and *S. damascena*, respectively.

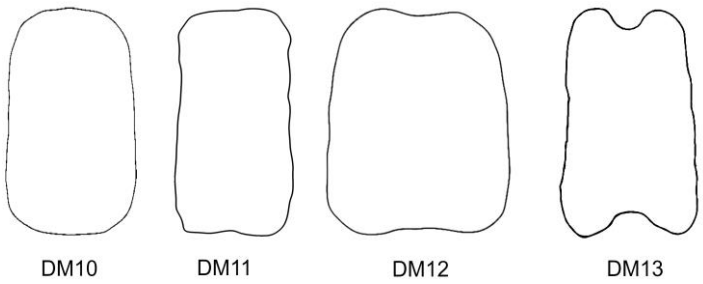

Figure 4. New dorsal models described in this work through the application of Fourier transform to average silhouettes as described [18].

3.4. Mean Values of J Index with 20 Seeds per species. Correspondence between the Lateral and Dorsal Views

J index values as the mean of 20 seeds were evaluated for lateral and dorsal views of all species with the best-fitting models. The models were selected after comparison of the results with the average silhouettes. A threshold was set at 89.0, such that species giving values lower than this threshold for the mean of 20 seeds for the lateral or dorsal view were discarded. The only exception was given to *S. damascena* with a *J* index of 86.5 in the dorsal view for the model DM13, due to the high specific shape of this model, which gives much lower values than any other species. A total of 24 species did not reach the established threshold value for the *J* index, in either lateral or dorsal models, or in both. These species correspond to 12 out of 33 in Table A2 (models DM2 and DM4), and 12 species in Table A3 (the rest of the lateral models). Regarding dorsal models, they correspond to: (i) a unique species in Table A4 (*S. perlmanii* W.L.Wagner, D.R.Herbst and Sohmer), (ii) 7 species in Table A5, and (iii) 16 out of the 17 species in Table A6 (all of them except *S. yunnanensis* Franch). Thus, the species giving low values of *J* indexes as the mean of 20 seeds are concentrated in the group of those whose average silhouettes gave best scores in models DM7 and DM9, which were the dorsal models more elongated and with concave regions at the poles. The remaining 27 species gave values of *J* indexes superior to 89.0 in both lateral and dorsal models, and will be the object of this section. Table 1 presents the *J* index values

obtained as mean values of 20 seeds for the lateral and dorsal models (LM and DM) in *E. coeli-rosa* and 27 species of *Silene*.

Table 1. Best scores obtained in lateral and dorsal models for each species of *Silene*, based on mean values of 20 seeds. Values of *J* index superior to 89.0 for the lateral and dorsal views are shown, except *S. damascena* for the dorsal model DM13.

Species	*J* Index (Lateral Model)	*J* Index (Dorsal Model)
S. marizii Samp.	90.9 (LM2)	91.4 (DM2)
S. petersonii Maguire	91.2 (LM2)	91.1 (DM2)
S. fruticosa L.	90.2 (LM2)	90.9 (DM3)
S. aprica Turcz. ex Fisch. and C.A. Mey	90.0 (LM2)	89.1 (DM10)
S. koreana Kom.	91.6 (LM2)	90.7 (DM10)
S. jeniseensis Willd.	90.8 (LM4)	89.2 (DM1)
S. hookeri Nutt.	91.2 (LM4)	90.2 (DM2)
S. virginica L.	90.7 (LM4)	89.4 (DM2)
S. baccifera (L.) Durande	91.7 (LM4)	89.8 (DM3)
S. chlorifolia Sm.	91.0 (LM4)	90 (DM5)
S. firma Siebold and Zucc.	91.0 (LM4)	91.2 (DM10)
S. nana Kar. and Kir.	91.8 (LM4)	92.2 (DM10)
S. chungtienensis (Speg.) Bocquet	90.8 (LM4)	89.9 (DM10)
S. fabaria (L.) Coyte	90.2 (LM4)	90.2 (DM10)
S. suksdorfii B.L. Rob.	89.3 (LM4)	91.5 (DM10)
S. viridiflora L.	90.7 (LM4)	91.3 (DM10)
S. yunnanensis Franch.	90.2 (LM4)	89.5 (DM11)
S. squamigera Boiss.subsp. *vesiculifera* (J.Gay ex Boiss.) Coode and Cullen	91.7 (LM5)	90.8 (DM6)
S. chlorantha (Willd.) Ehrh.	90.8 (LM5)	89.5 (DM11)
S. longicilia (Brot.) Otth	90.6 (LM5)	89.4 (DM11)
S. pygmaea Adams	90.2 (LM5)	89.0 (DM11)
S. linicola C.C. Gmel.	90.6 (LM5)	89.7 (DM12)
S. damascena Boiss. and Gaill.	91.6 (LM5)	86.5 (DM13)
S. villosa Forssk.	91.4 (LM8)	91.5 (DM5)
S. dichotoma Ehrh.	90.6 (LM8)	89.6 (DM10)
S. integripetala Bory and Chaub.	89.1 (LM8)	89.4 (DM10)
S. multiflora (Erhr.) Pers.	90.2 (LM8)	90.7 (DM10)
E. coeli-rosa (L.) Fenzl ex Endl.	89.8 (LM5)	90 (DM10)

The seed images of five *Silene* species gave good scores in LM2 and some other dorsal models (Table 1). Among them, both *S. marizii* and *S. petersonii* adjusted to LM2 and DM2 best (Figure 5), the species *S. fruticosa* to LM2 and DM3 (Figure 6); and, finally, the two species *S. aprica* and *S. koreana* to LM2 and DM10 (Figure 7).

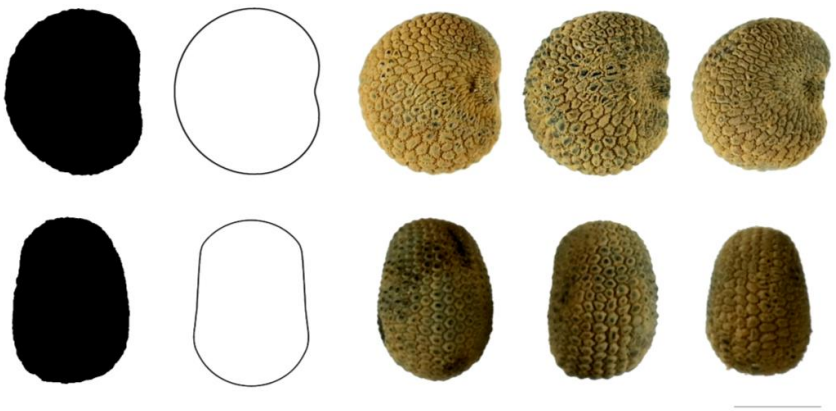

Figure 5. *Silene marizii*: average silhouettes (left), the models giving best scores with 20 seeds (LM2 and DM2), and three representative images for the lateral (above) and dorsal (below) seed views. Bar represents 1 mm.

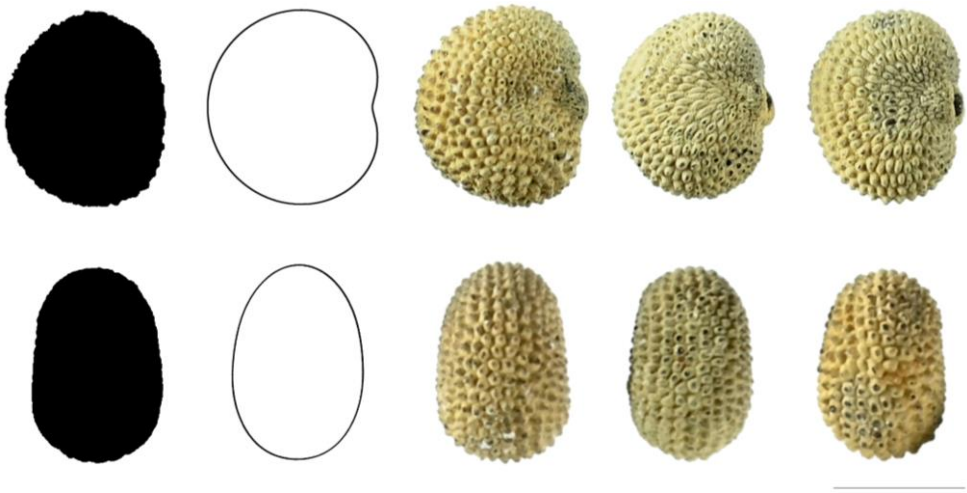

Figure 6. *Silene fruticosa*: average silhouettes (left), the models giving best scores with 20 seeds (LM2 and DM3), and three representative images for the lateral (above) and dorsal (below) seed views. Bar represents 1 mm.

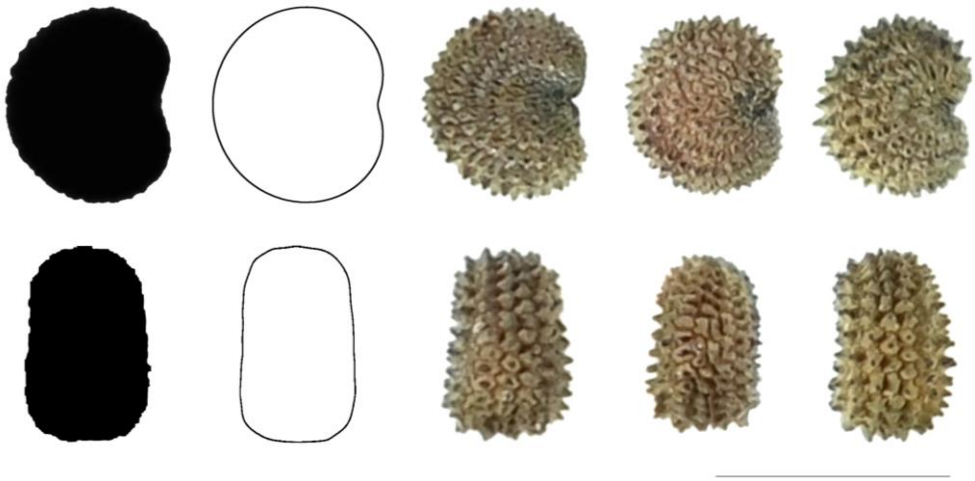

Figure 7. *Silene aprica*: average silhouettes (left), the models giving best scores with 20 seeds (LM2 and DM10), and three representative images for the lateral (above) and dorsal (below) seed views. Bar represents 1 mm.

Twelve species gave the best scores in the model LM4, but the dorsal models were different for some of them (Table 1). The seeds of four species adjusted well to convex models DM1 to DM3. The seeds of *S. jeniseensis* adjusted to LM4 and DM1 (Figure 8), those of *S. hookerii* and *S. virginica* to LM4 and DM2 (Figure 9), and those of *S. baccifera,* to LM4 and DM3 (Figure 10). Only the seeds of *S. chlorifolia* presented the combination of LM4 and DM5 (Figure 11). Six species (*S. chungtienensis*, *S. fabaria, S. firma, S. nana, S. suksdorfii*, and *S. viridiflora*) shared the same model combination of LM4 and DM10 (Figure 12), while *S. yunnanensis* was the only species with a combination between LM4 and DM11 (Figure 13).

Regarding model LM5, only the seeds of *S. squamigera* subsp. *vesiculifera* showed an association between LM5 and DM6 (Figure 14); in contrast, *S. chlorantha, S. longicilia,* and *S. pygmaea* showed a similarity to DM11 (Figure 15), *S. linicola* to DM12 (Figure 16), and *S. damascena* to DM13 (Figure 17).

Four *Silene* species gave good *J* index values in model LM8, and two models DM5 and DM10. Just as *S. villosa* showed the combination of LM8 and DM5 (Figure 18), the combination for *S. dichotoma, S. integripetala*, and *S. multiflora* was with DM10 (Figure 19). Finally, the seeds of *E. coeli-rosa* adjusted well to models LM5 and DM10 (Figure 20).

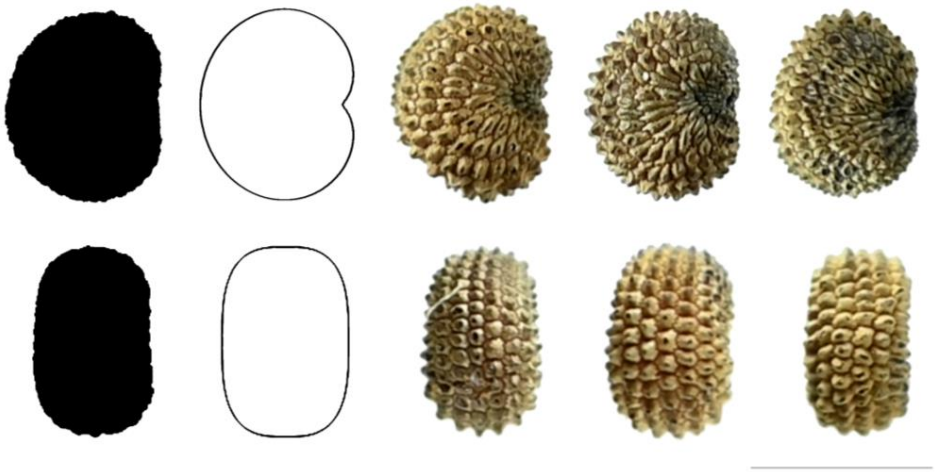

Figure 8. *Silene jeniseensis*: average silhouettes (left), the models giving best scores with 20 seeds (LM4 and DM1), and three representative images for the lateral (above) and dorsal (below) seed views. Bar represents 1 mm.

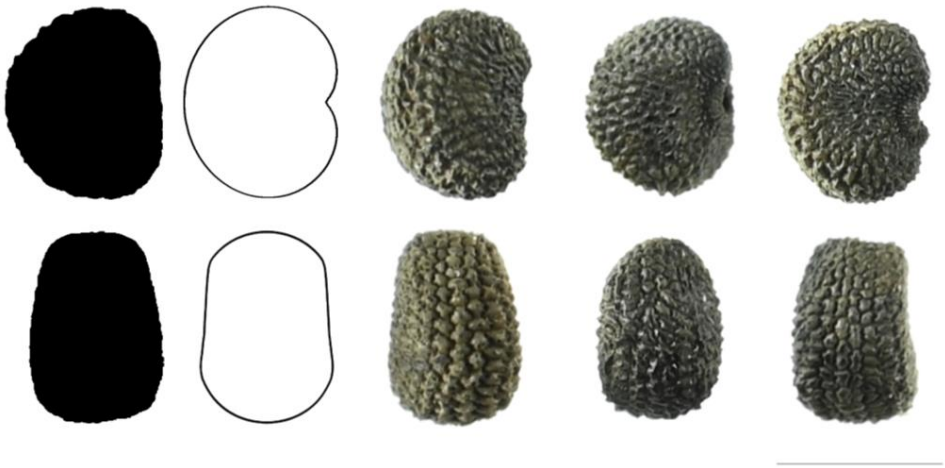

Figure 9. *Silene hookeri*: average silhouettes (left), the models giving best scores with 20 seeds (LM4 and DM2), and three representative images for the lateral (above) and dorsal (below) seed views. Bar represents 1 mm.

Figure 10. *Silene baccifera*: average silhouettes (left), the models giving best scores with 20 seeds (LM4 and DM3), and three representative images for the lateral (above) and dorsal (below) seed views. Bar represents 1 mm.

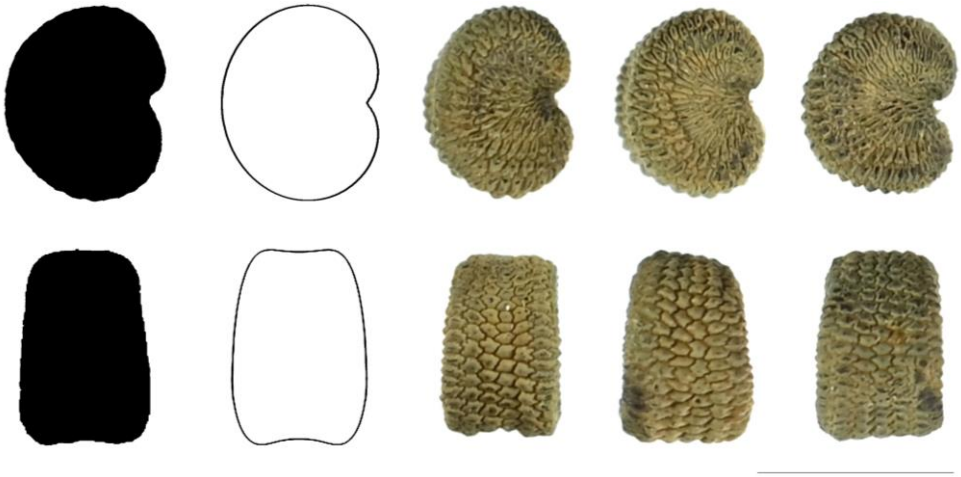

Figure 11. *Silene chlorifolia*: average silhouettes (left), the models giving best scores with 20 seeds (LM4 and DM5), and three representative images for the lateral (above) and dorsal (below) seed views. Bar represents 1 mm.

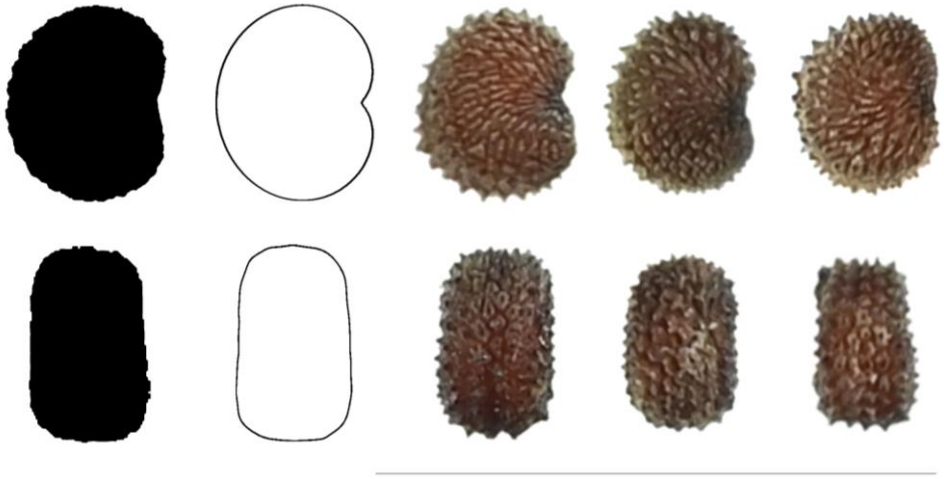

Figure 12. *Silene chungtienensis*: average silhouettes (left), the models giving best scores with 20 seeds (LM4 and DM10), and three representative images for the lateral (above) and dorsal (below) seed views. Bar represents 1 mm.

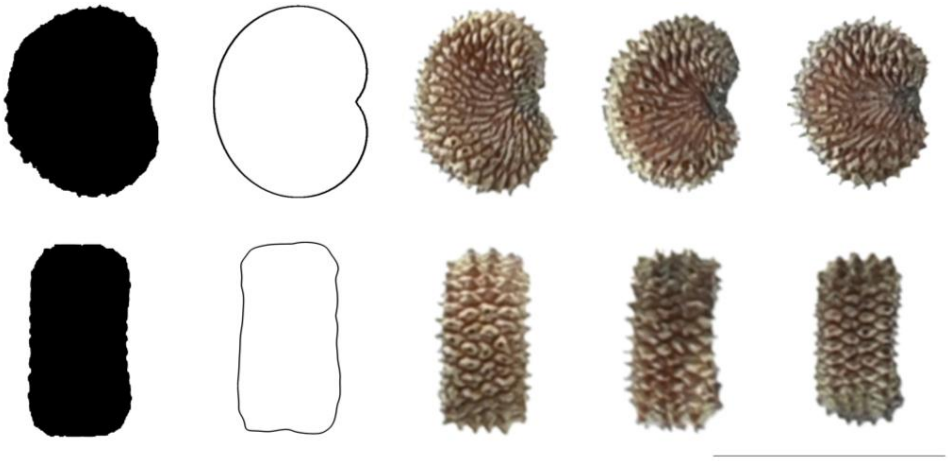

Figure 13. *Silene yunnanensis*: average silhouettes (left), the models giving best scores with 20 seeds (LM4 and DM11), and three representative images for the lateral (above) and dorsal (below) seed views. Bar represents 1 mm.

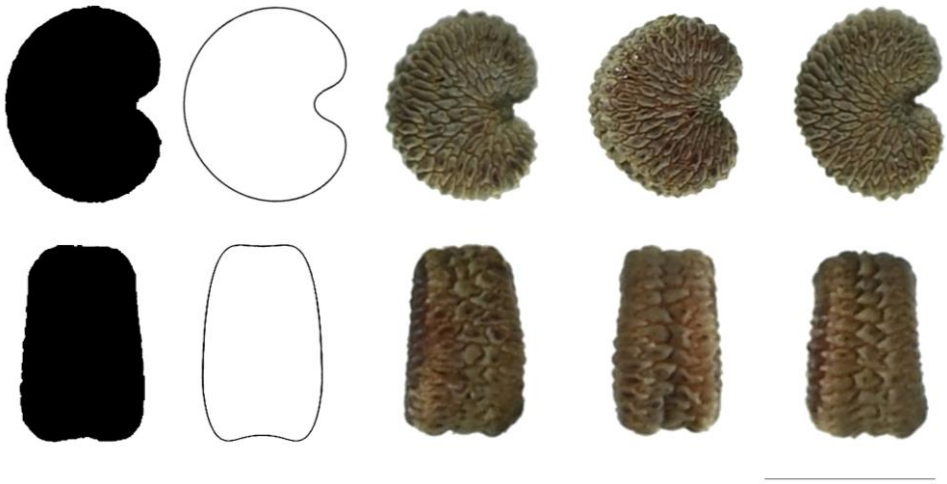

Figure 14. *Silene squamigera* subsp. *vesiculifera*: average silhouettes (left), the models giving best scores with 20 seeds (LM5 and DM6), and three representative images for the lateral (above) and dorsal (below) seed views. Bar represents 1 mm.

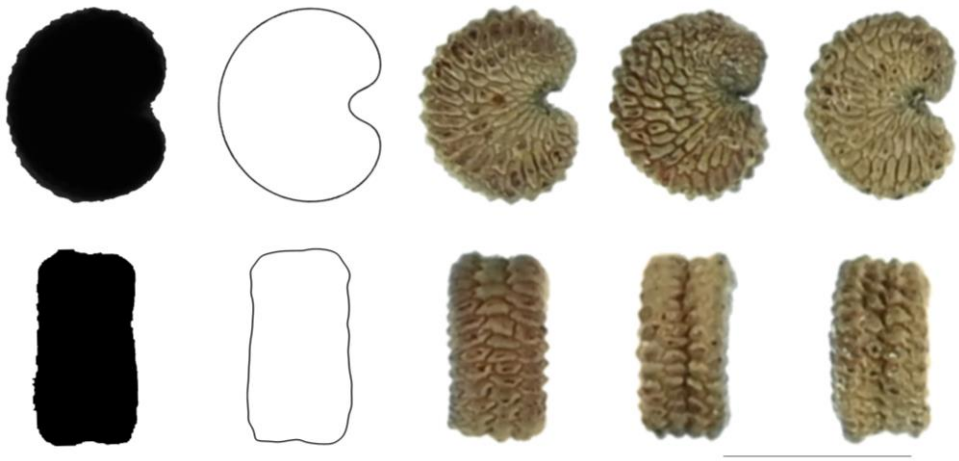

Figure 15. *Silene chlorantha*: average silhouettes (left), the models giving best scores with 20 seeds (LM5 and DM11), and three representative images for the lateral (above) and dorsal (below) seed views. Bar represents 1 mm.

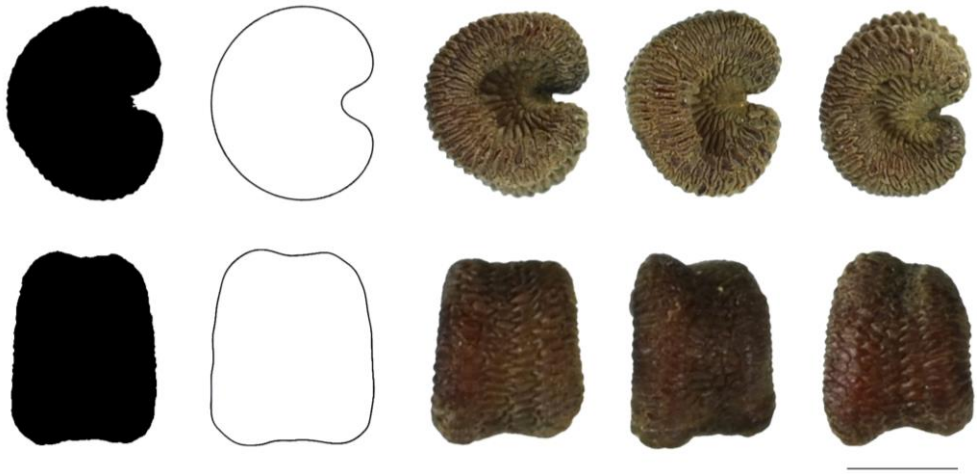

Figure 16. *Silene linicola*: average silhouettes (left), the models giving best scores with 20 seeds (LM5 and DM12), and three representative images for the lateral (above) and dorsal (below) seed views. Bar represents 1 mm.

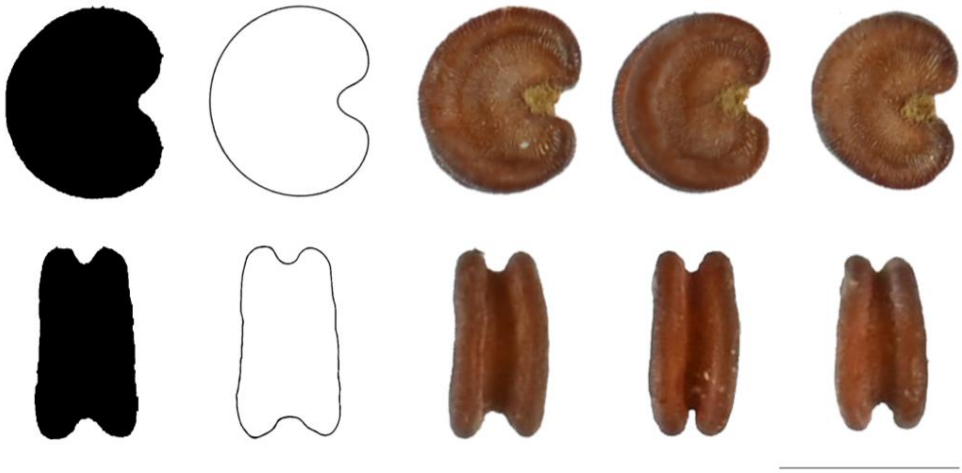

Figure 17. *Silene damascena*: average silhouettes (left), the models giving best scores with 20 seeds (LM5 and DM13), and three representative images for the lateral (above) and dorsal (below) seed views. Bar represents 1 mm.

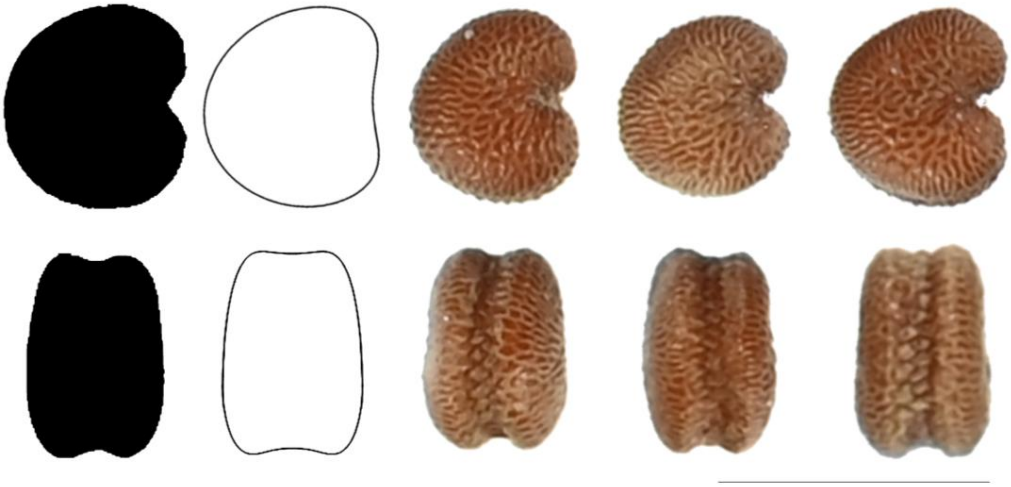

Figure 18. *Silene villosa*: average silhouettes (left), the models giving best scores with 20 seeds (LM8 and DM5), and three representative images for the lateral (above) and dorsal (below) seed views. Bar represents 1 mm.

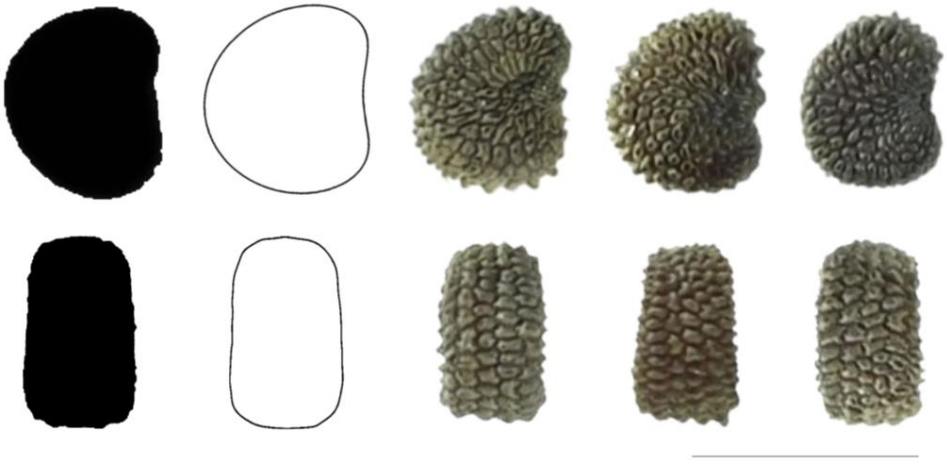

Figure 19. *Silene multiflora*: average silhouettes (left), the models giving best scores with 20 seeds (LM8 and DM10), and three representative images for the lateral (above) and dorsal (below) seed views. Bar represents 1 mm.

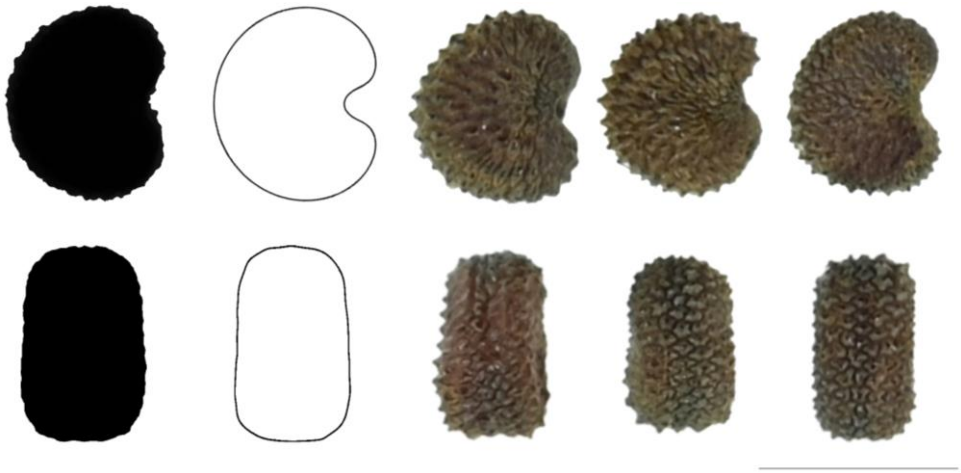

Figure 20. *Eudianthe coeli-rosa*: average silhouettes (left), the models giving best scores with 20 seeds (LM5 and DM10), and three representative images for the lateral (above) and dorsal (below) seed views. Bar represents 1 mm.

3.5. The Relationship between Geometric Models and Taxonomic Sections

The dendrogram in Figure 21 shows the relationship between *Silene* species based on seed morphology. The results confirm and expand a certain relationship between the morphological groups obtained by the comparison with models and the current taxonomy of *Silene*. Species in *S.* subgen. *Behenantha* have more convex seeds corresponding to models LM2/LM4. In contrast, the models with large concavities, such as LM5, define better the shape of seeds in the species of *S.* sect. *Silene* in subg. *Silene*. Further analyses will be needed, including new models to better define the relationships between species.

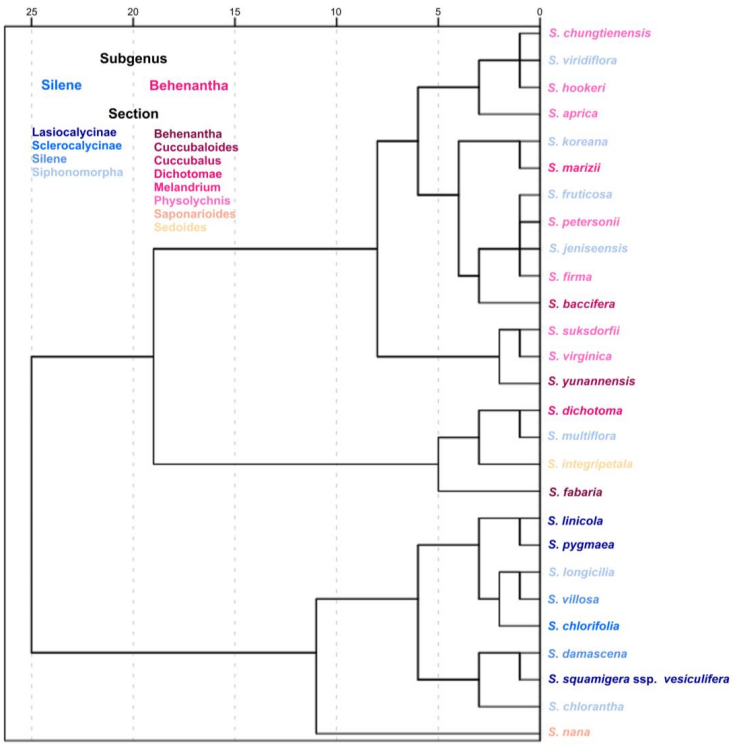

Figure 21. Dendrogram based on hierarchical clustering with the values of *J* index obtained from the analysis with lateral models LM2/4 and LM5. Species of subg. *Behenantha* are concentrated in the upper part of the diagram, while species of subg. *Silene* are grouped in the lower branches, excluding those species of sec. *Siphonomorpha*, that are scattered through the dendrogram. Results are shown for the 27 species of Table 1.

4. Discussion

The similarity of lateral views of *Silene* seeds with the cardioid led to the application of geometric models in the quantification of seed shape. In general, the mean value of the *J* index obtained with the cardioid (LM1) in seeds of species of *S.* subg. *Behenantha* was higher than in seeds of *S.* subg. *Silene* [14]. Nevertheless, the description of other, additional geometric models derived from the cardioid gave better *J* index values when applied to the species of *S.* subg. *Silene* (e.g., LM3 for *S. gallica,* LM6 for *S. mellifera,* LM5 for *S. tridentata*). The same trend applied to the species of *S.* subg. *Behenantha* (e.g., LM2 for *S. latifolia*, LM4 for *S. diclinis*) [14,15].

In general, the combination of models LM2 to LM8 may be more discriminant than the cardioid (LM1) itself, because they narrow better the morphological characteristics of seeds (open or closed in the hilum region). Geometric models LM2, LM4, and LM8 corresponded to those seeds with a more plane and closed region around the hilum, characterized by low partial concavities and high solidity [12]. Meanwhile, models LM3, LM5, LM6, and LM7 presented an open region (partial concavity) in the hilum region [14,15]. Thus, both groups represent alternative morphologies. In addition, the dorsal view of seeds was also analyzed to provide quantitative data about shape and morphology from this view [16]. The application of new models for the dorsal views showed that convex models adjusted better to seed images of *S.* subg. *Behenantha* [16]. On the contrary, we have seeds with partial concavities in the upper and lower sides of their dorsal views due to a channel running through the profile of the seed. These are known as *dorso canaliculata* [1–3] and correspond to non-convex models in their dorsal views, such as *S. apetala*, *S. colorata* Poir., *S. inaperta*, or *S. ramosissima.* They are frequently present in *S.* subg. *Silene*, and less common or absent in some sections of *Silene* subg. *Behenantha*, such as *Silene* sect. *Melandrium* [16].

These results suggest that the comparison with geometric figures might be a useful tool to apply morphological traits in plant taxonomy. Hence, an important question for the consideration of the taxonomic value of these morphological characters based on geometric models concerns their stability. Although these geometric models revealed levels of stability for certain complex taxonomic groups of *Silene* [12–18], more data are still needed to fully support these previous statements.

In this work, we have classified 51 species of *Silene* from diverse geographic provenances. The classification was according to their highest scores of *J* index values with specific geometric models for their lateral and dorsal views. The analysis started with the values of the *J* index in the average silhouettes for the lateral and dorsal view of each species. Average silhouettes gave a preliminary approximation to overall seed shape in both views, lateral and dorsal [15–17]. They provide information about aspects of seed morphology such as general symmetry, aspect ratio, and convexity. For example, the seeds of eight species resembling model LM5 show positive correspondence in DM5 to DM9, but it is negative in models DM1–DM4. A total of 10 species giving strong similarity in their average silhouettes for the dorsal views with convex models (DM1–DM4) belong to the group of high similarity with convex models LM2 and LM4. Likewise, non-convex models DM8 and DM9 are linked to the group of 17 species which are elongated and gave low results of *J* indexes in the tests based on mean values of 20 seeds. All of them, except *S. yunnanensis*, were discarded from further study. This might indicate that these seeds require more specific models or that their seeds were quite heterogenous. Nevertheless, elevated values of aspect ratio (elongated seeds) could be a symptom of dehydration due to prolonged storage or storage in adverse conditions [22].

We found an association between the *J* index in the average silhouettes and the *J* index as the mean value of 20 individual seeds. The group of species whose average silhouettes gave higher scores in LM2, LM4, and LM8 contains all the species giving the best scores in these models when estimated as means of 20 seeds. Similarly, most species giving elevated scores of *J* index as the mean value of 20 individual silhouettes in LM5 (e.g., *S. linicola*, *S. longicilia*, *S. pygmaea*, and *S. damascena*) also had high values in this model in their average silhouettes. Values obtained with average silhouettes, although indicative of seed shape

in a group of seeds, could give overestimations because the analyses with the average silhouettes concentrate more on conserved regions, and hence, the shape of many seeds can differ from their corresponding average silhouette. Thus, the final analysis including *J* index values measured as the mean of 20 seeds results in much more precise estimations.

A protocol based on Fourier transform allows us to define models according to their shape, independently of known geometric figures [18]. The protocol has been applied here to design the new dorsal models DM10 to DM13. Among them, DM10 is convex while the other three models present regions of variable concavities. DM10 fits well for the dorsal view in 11 species. All of them combined with LM2, LM4, or LM8: *S. aprica* and *S. koreana* (LM2), *S. firma, S. nana, S. chungtienensis*, *S. fabaria*, *S. suksdorfii*, and *S. viridiflora* (LM4), and *S. dichotoma*, *S. integripetala*, and *S. multiflora* (LM8). This result would confirm the hypothesis that convex models in the dorsal view are associated with convex models in the lateral view [16]. Most of these 11 species, whose seeds adjust to convex models, belong to *S.* subg. *Behenantha.* Model DM11, with small concavity regions, applies also to a variety of species in combination with both convex for LM4 in *S. yunnanensis*, and non-convex for LM5 in *S. chlorantha*, *S. longicilia*, and *S. pygmaea*. In contrast to DM10 and DM11, the new models DM12 and DM13 with larger concavity regions are highly specific for *S. linicola* and *S. damascena*, both combined in LM5, a lateral model presenting a large concavity in the hilum region.

When considering *J* index values obtained as the mean of 20 measurements, the combination between lateral models closed in the hilum (LM2, LM4, and LM8) and convex models (DM1–DM4, and DM10) was conserved in 18 species: (i) 13 of S. subg. *Behenantha*: *S. aprica*, *S. baccifera, S. chungtienensis, S. dichotoma, S. fabaria, S. firma, S. hookeri, S. jeniseensis, S. marizii, S. nana, S. petersonii, S. suksdorfii*, and *S. virginica;* and (ii) 5 of *S.* subg. *Silene*: *S. fruticosa, S. jeniseensis, S. koreana, S. multiflora,* and *S. viridiflora*. These latter five species belong to *Silene* sect. *Siphonomorpha*. On the other hand, the combination of lateral models more open in the hilum (LM5) and dorsal models with concavities is more frequent in species of *S.* subg. *Silene.* The six species adjusting to LM5 belong to this group: *S. squamigera* subsp. *vesiculifera*, *S. chlorantha, S. longicilia*, *S. pygmaea, S. linicola*, and *S. damascena*. From these, one adjusts to DM6 (*S. squamigera* subsp. *vesiculifera*), while five of them adjust to the newly designed models DM11 (*S. chlorantha, S. longicilia*, *S. pygmaea*), DM12 (*S. linicola*), and DM13 (*S. damascena).*

The cardioid (reniform or kidney-shaped) shape of the seeds is associated with the campylotropous ovule, with most of the morphological axis curved, allowing a great morphological variety in ovules and seeds [23], which is associated with various types of asymmetries [14]. Consequently, the similarity of seeds with the cardioid is limited to some *Silene* species, while others require specific models for accurate description and quantification. The application of Fourier transform allows the description of new, specific models for these seed images that do not adjust well to defined geometrical figures.

New species of *Silene* are regularly being described [24–26], and the taxonomy of this genus is being revised [27–29]. Having the genus *Silene* in mind, we present protocols based on seed morphology, which represent a new technique to contribute to this objective. These protocols may be applied with optical photographic equipment and image analysis programs.

5. Conclusions

The analyses of seed morphology in 51 new *Silene* species and the close-related species *Eudianthe coeli-rosa* by lateral and dorsal models revealed the existence of a robust behavior between species and geometric models. In addition, there is a remarkable correspondence between certain lateral and dorsal models. Those lateral models closed in the hilum region (LM2 and LM4) were associated with convex dorsal models (DM1–DM4, and DM10). Conversely, those lateral geometric models more open in the hilum region were well adapted to seeds with partial concavities in their dorsal views (mostly *dorso canaliculata*

seed types). The former correspond to species in *Silene* subg. *Behenantha*, while the later are associated with particular sections in *S.* subg. *Silene*.

Supplementary Materials: A video describing the method for obtaining the average silhouette in a seed image sample is available at (https://zenodo.org/record/4478344#.YzxbmExBxD8). The seed images used in the analysis are stored available (https://zenodo.org/record/7330942#.Y3Y8Hn3MJD8). The Mathematica code for the new models DM10–DM13 are available (https://zenodo.org/record/7386404#.Y4ipln3MJD8). The three items were accessed on 13 December 2022.

Author Contributions: Conceptualization, E.C.; methodology, E.C. and J.J.M.-G.; software, J.J.M.-G. and J.L.R.-L.; validation, J.J.M.-G., J.L.R.-L., B.J., A.J. and E.C.; formal analysis, J.J.M.-G., J.L.R.-L., B.J., A.J. and E.C.; investigation, J.J.M.-G., J.L.R.-L., B.J., A.J. and E.C.; resources, J.J.M.-G., J.L.R.-L., B.J., A.J. and E.C.; data curation, J.J.M.-G.; writing—original draft preparation, E.C.; writing—review and editing, J.J.M.-G., J.L.R.-L., B.J., A.J. and E.C.; visualization, J.J.M.-G. and E.C.; supervision, E.C.; project administration, E.C.; funding acquisition, E.C. All authors have read and agreed to the published version of the manuscript.

Funding: This research was funded by Project "CLU-2019-05-IRNASA/CSIC Unit of Excellence", funded by the Junta de Castilla y León and co-financed by the European Union (ERDF "Europe drives our growth").

Institutional Review Board Statement: Not applicable.

Informed Consent Statement: Not applicable.

Data Availability Statement: Not applicable.

Acknowledgments: We thank Elena Estrelles and the Carpoespermateca of the botanical garden at the University of Valencia for providing the seeds used in this study.

Conflicts of Interest: The authors declare no conflict of interest.

Appendix A

Table A1. Seeds of the genera *Eudianthe* and *Silene* used in this work, with the indication of the source and origin of the samples, based on the information given from the seed collection of the botanical garden of the University of Valencia (Spain). The name of the subgenus and the corresponding sections (between brackets) are indicated.

Species	Source	Place of Origin	Subgenus (Section)
Eudianthe coeli-rosa (L.) Fenzl ex Endl.	Jardin Botanique de la ville de Lyon	Haute-Corse (2B), Désert des Agriates, plage de Loto	-
Silene aprica Turcz. ex Fisch. and C.A. Mey.	Chollipo Arboretum	Botanical Garden	*Behenantha* (*Physolychnis*)
S. baccifera (L.) Durande	Kärntner Botanikzentrum	Kärnten: Grafenstein, Sabuatach, glade *Pinus sylvestris* forest, on conglomerate, 615 m (19.8.2012)	*Behenantha* (*Cuccubalus*)
S. bupleuroides L.	Hortus Botanicus Vacratot, Hungary	-	*Silene* (*Sclerocalycinae*)
S. caryophylloides (Poir.) Otth	Botanischer Garten der Universität Tübingen	Holubec; Turkei, Ulu Dag	*Silene* (*Auriculatae*)
S. chlorantha (Willd.) Ehrh.	Botanischer Garten der Universität Potsdam	Germany. Brandenburg, Odergebiet, an der Bahn, SW Bahnhof Podelzig	*Silene* (*Siphonomorpha*)
S. chlorifolia Sm.	BG der Martin-Luther-Univ. Halle-Wittenberg	-	*Silene* (*Sclerocalycinae*)
S. chungtienensis (Speg.) Bocquet	Botanic Garden of the University of Copenhagen	-	*Behenantha* (*Physolychnis*)
S. ciliata Pourr.	Botany Hung. Acad. of Sciences	Botanical Garden	*Silene* (*Silene*)
S. damascena Boiss. and Gaill.	The Botanical Garden Tel Aviv University	Mount Hermon	*Silene* (*Silene*)
S. dichotoma Ehrh.	Botanic Garden of the University of Copenhagen	-	*Behenantha* (*Dichotomae*)
S. dinarica Spreng.	Botanicka Zahrada Teplice	-	*Silene* (*Siphonomorpha*)

Table A1. *Cont.*

Species	Source	Place of Origin	Subgenus (Section)
S. fabaria (L.) Coyte	Botanischer Garten der Universität Bonn	Chakidiki, south of Ouranopolis, towards the border of Athos	*Behenantha* (*Behenantha*)
S. firma Siebold and Zucc.	The Hiroshima Botanical Garden	North-western Hiroshima pref., a pass near the mountain, 800 m, Oct 2014	*Behenantha* (*Physolychnis*)
S. foliosa Maxim.	Vladivostok Botanical Garden	Gamow Peninsula	*Silene* (*Siphonomorpha*)
S. frivaldskyana Hampe	Siberian Botanical Garden of Tomsk State University	-	*Silene* (*Siphonomorpha*)
S. fruticosa L.	Jardin Botanique de Dijon	-	*Silene* (*Siphonomorpha*)
S. gigantea (L.) L.	Julia and Alexander N. Diomides Botanic Garden	Cult./ATHD	*Silene* (*Siphonomorpha*)
S. hayekiana Hand.-Mazz. and Janch.	University Botanic Gardens Ljubljana	Mazzeti and Janchen—Kucelj	*Silene* (*Siphonomorpha*)
S. holzmani Heldr. ex Boiss.	Julia and Alexander N. Diomides Botanic Garden	Spont./Glaronisi islet-Pigadia-Karpathos Island	*Behenantha* (*Behenantha*)
S. hookeri Nutt.	Botanicka Zahrada Teplice	-	*Behenantha* (*Physolychnis*)
S. integripetala Bory and Chaub.	BG der Martin-Luther-Univ. Halle-Wittenberg	-	*Behenantha* (*Sedoides*)
S. jeniseensis Willd.	Vladivostok Botanical Garden	Gamow Peninsula	*Silene* (*Siphonomorpha*)
S. koreana Kom.	Botanic Garden of Perm State University	-	*Silene* (*Siphonomorpha*)
S. laciniata Cav.	The Medicinal Herb Garden, University of Washington	-	*Behenantha* (*Physolychnis*)
S. legionensis Lag.	BG Universidade de Coimbra	Alimonde–Bragança	*Silene* (*Silene*)
S. linicola C.C. Gmel.	Jardin Botanique de la ville de Lyon	Aube (10), entre Auxerre et Troyes	*Silene* (*Lasiocalycinae*)
S. longicilia (Brot.) Otth	BG Universidade de Coimbra	Serra da Boa Viagem–Figueira da Foz	*Silene* (*Siphonomorpha*)
S. magellanica (Desr.) Bocquet	Station Alpine du Lautaret. Univ. Joseph Fourier	Punta Arenas (Chili, 10 m)	*Behenantha* (*Physolychnis*)
S. marizii Samp.	BG Universidade de Coimbra	Nespereira–Celorico da Beira	*Behenantha* (*Melandrium*)
S. multicaulis Guss. subsp. *multicaulis*	Bundesgärten Alpengarten im Belvedere (Viena, Austria)	-	*Silene* (*Siphonomorpha*)
S. multiflora (Erhr.) Pers.	Botany Hung. Acad. of Sciences	Botanical Garden	*Silene* (*Siphonomorpha*)
S. nana Kar. and Kir.	National Botanical Garden of Iran	Arak, 20 km to Borujerd, Robatmil to Chepeghli village	*Behenantha* (*Saponarioides*)
S. paradoxa L.	Station Alpine du Lautaret. Univ. Joseph Fourier	Défilé d'Inzecca (Corse, 250 m)	*Silene* (*Siphonomorpha*)
S. perlmanii W.L.Wagner, D.R.Herbst and Sohmer	Botanischer Garten der Universität Zürich	-	*Silene* (*Sclerophyllae*)
S. petersonii Maguire	BG der Martin-Luther-univ. Halle-Wittenberg	Mount Brocken Garden	*Behenantha* (*Physolychnis*)
S. pomelii Batt. subsp. *adusta* (Ball) Maire	Station Alpine du Lautaret. Univ. Joseph Fourier	Essaouira (Maroc), 0 m	*Silene* (*Silene*)
S. pygmaea Adams	St Andrews Botanical Garden	-	*Silene* (*Auriculatae*)
S. regia Sims	Botanischer Garten Universität Hamburg	Nachzucht BG Hamburg (Winona, MN/US; Prairie Moon Nursery)	*Behenantha* (*Physolychnis*)
S. roemeri Friv.	St Andrews Botanical Garden	-	*Silene* (*Siphonomorpha*)
S. samojedorum (Sambuk) Oxelman	Hortus Botanicus Patavinus	-	*Behenantha* (*Physolychnis*)
S. saxatilis Sims	Botanischer Garten München-Nymphenburg	Georgia, Reg. Guria, cerca de Bakhmaro. 1950 m	*Silene* (*Siphonomorpha*)
S. spinescens Sm.	Julia and Alexander N. Diomides Botanic Garden	Spont./Sounion National Park-Attiki	*Silene* (*Siphonomorpha*)
S. squamigera Boiss. subsp. *vesiculifera* (J.Gay ex Boiss.) Coode and Cullen	Botanic Garden of the University of Copenhagen	-	*Silene* (*Lasiocalycinae*)
S. suksdorfii B.L. Rob.	Botanischer Garten München-Nymphenburg	-	*Behenantha* (*Physolychnis*)
S. swertiifolia Boiss.	National Botanical Garden of Iran	Elam, Before the tunnel Javar	*Silene* (*Sclerocalycinae*)
S. vallesia L. subsp. vallesia	Station Alpine du Lautaret. Univ. Joseph Fourier	Villar d'Arène, 1700 m	*Silene* (*Auriculatae*)
S. villosa Forssk.	The Botanical Garden Tel Aviv University	-	*Silene* (*Silene*)
S. virginica L.	Botanischer Garten Universität Hamburg	US: North Carolina; Burke County (USA-Reise 2013)	*Behenantha* (*Physolychnis*)
S. viridiflora L.	Gradina Botanica "Alexandru Borza" Cluj-Napoca Romania	Botanical Garden	*Silene* (*Siphonomorpha*)
S. waldsteinii Griseb.	Göteborg Botanical Garden	Greece, Florinis, Mt. Voras	*Silene* (*Siphonomorpha*)
S. yunnanensis Franch.	Botanischer Garten der Universität Zürich	-	*Behenantha* (*Cucubaloides*)

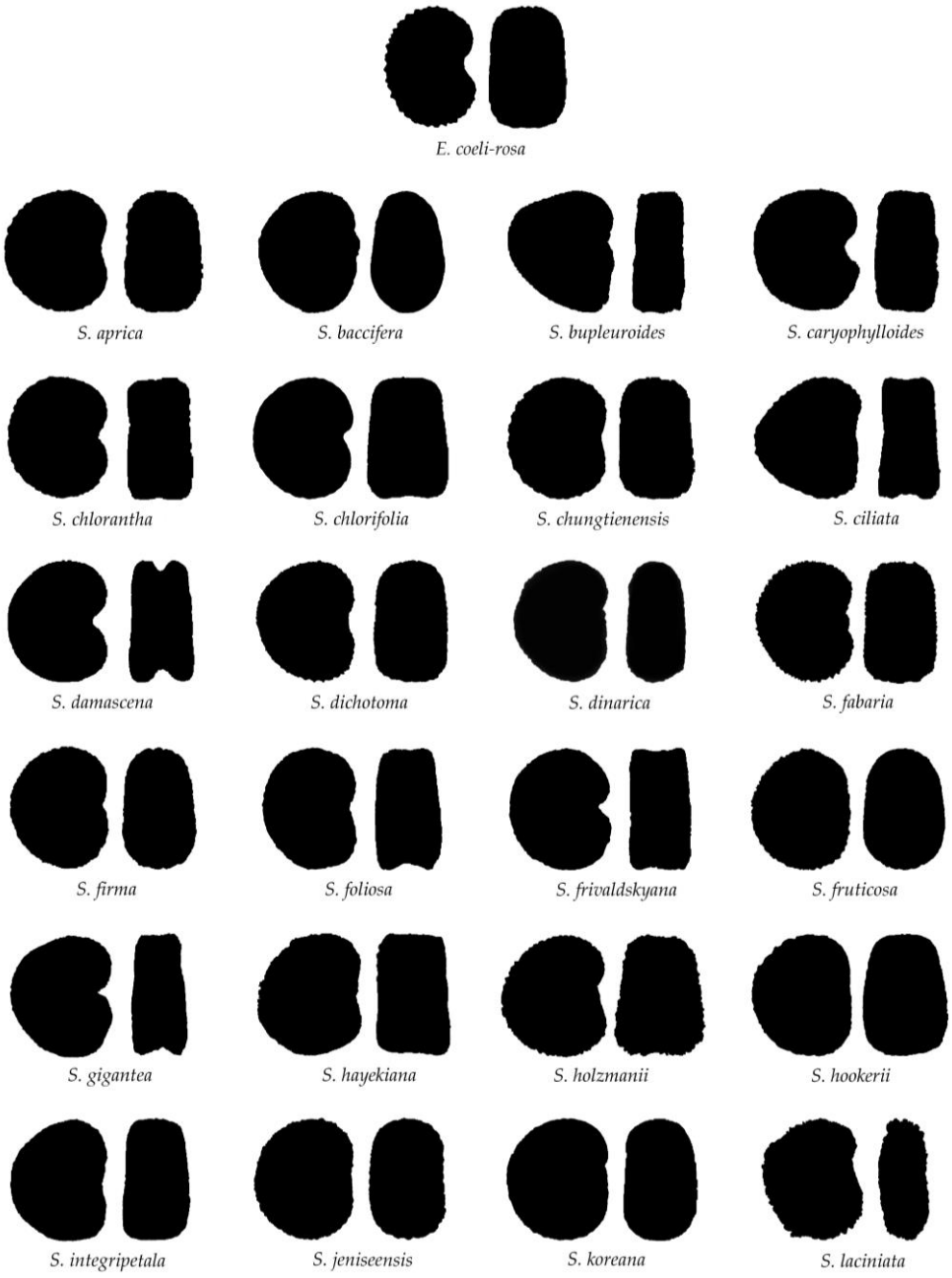

Figure A1. *Cont*.

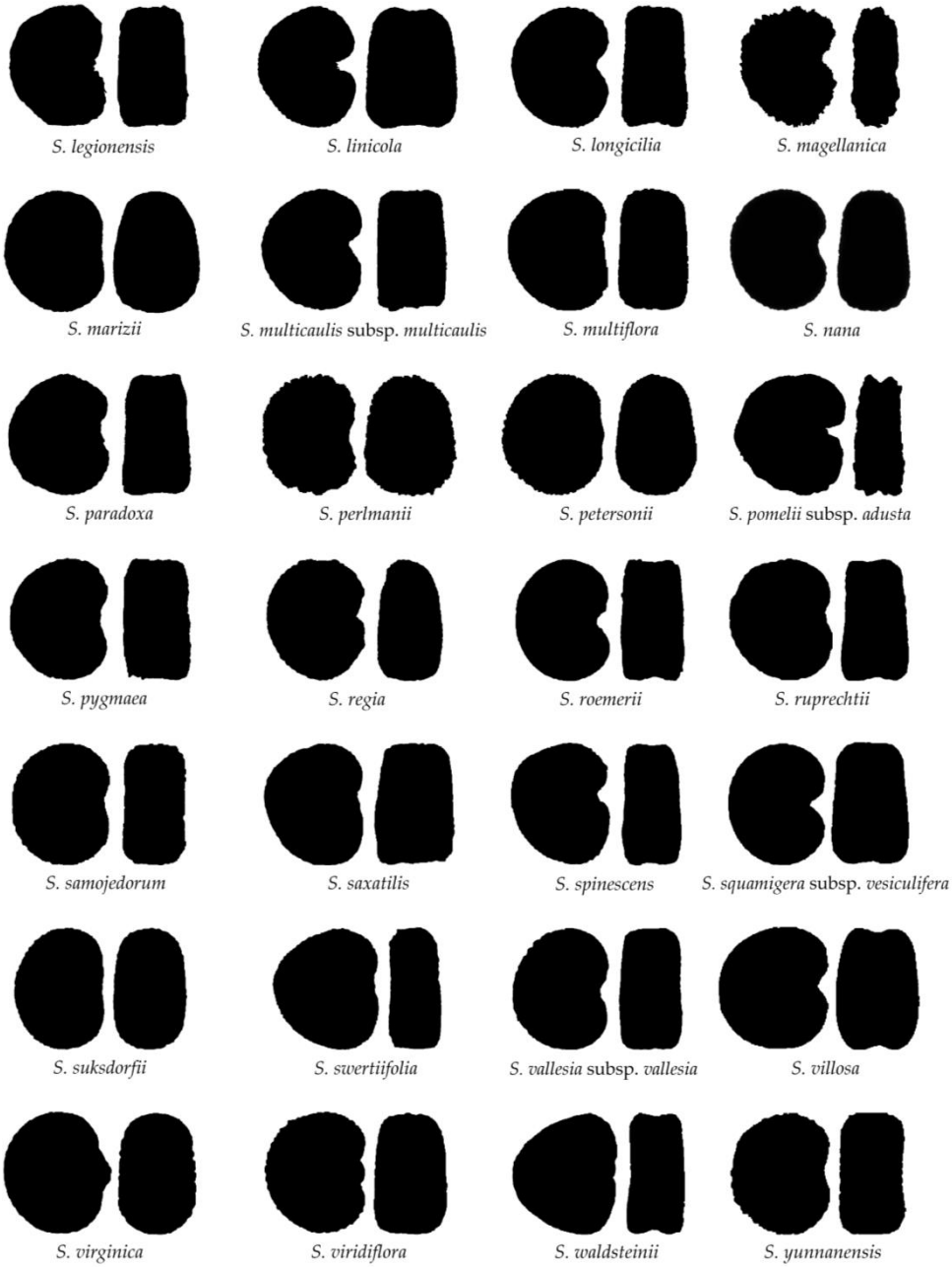

Figure A1. Average silhouettes for the species of *Silene* and *Eudianthe*, the object of this work.

Table A2. Values of *J* index for the average silhouettes of each species with the eight lateral models: species giving higher values in models LM2, LM4, or LM8 than in other models. In bold: species that did not reach the threshold value of 89.0 for the *J* index estimated as the mean of 20 seeds. B: corresponds to *S*. subg. *Behenantha*; S: corresponds to *S*. subg. *Silene*.

Species	Subgenus (Section)	LM1	LM2	LM3	LM4	LM5	LM6	LM7	LM8
S. aprica	B (*Physolychnis*)	93.8	93.4	88.0	92.0	92.9	84.4	91.9	91.7
S. baccifera	B (*Cuccubalus*)	91.8	92.4	88.5	92.6	88.6	85.8	88.1	89.3
S. bupleuroides	S (*Sclerocalycinae*)	85.6	86.1	81.6	84.4	84.3	79.1	86.0	90.4
S. chlorantha	S *(Siphonomorpha)*	93.0	91.8	87.6	93.6	92.8	84.2	90.3	90.1
S. chlorifolia	S *(Sclerocalycinae)*	92.4	91.8	89.2	94.0	92.8	85.8	90.2	90.4
S. chungtienensis	B (*Physolychnis*)	92.6	92.0	89.4	94.0	92.3	86.5	89.9	90.8
S. ciliata	S *(Silene)*	88.2	87.7	84.6	87.3	86.6	83.7	89.7	92.2
S. dichotoma	B *(Dichotomae)*	90.9	90.1	89.5	91.6	91.7	87.1	90.8	89.1

Table A2. *Cont.*

Species	Subgenus (Section)	LM1	LM2	LM3	LM4	LM5	LM6	LM7	LM8
S. dinarica	S *(Siphonomorpha)*	89.1	88.6	90.2	91.6	89.0	89.0	87.9	88.2
S. gigantea	S *(Siphonomorpha)*	91.2	89.9	89.1	90.7	91.1	85.9	90.3	91.2
S. hayekiana	S *(Siphonomorpha)*	90.6	89.7	86.0	89.9	89.1	82.8	88.4	92.9
S. holzmannii	B *(Behenantha)*	92.9	91.9	86.8	89.8	91.1	82.9	91.8	93.7
S. fabaria	B *(Behenantha)*	91.1	90.8	88.3	92.4	91.8	87.5	89.8	88.7
S. firma	B (*Physolychnis*)	92.7	92.2	89.3	94.2	91.2	87.0	89.5	91.0
S. foliosa	S *(Siphonomorpha)*	88.4	87.6	89.7	92.3	90.2	88.4	87.4	86.7
S. frivaldskyana	S *(Siphonomorpha)*	93.1	92.3	88.7	93.4	91.0	85.5	90.0	89.6
S. fruticosa	S *(Siphonomorpha)*	92.8	93.2	87.0	93.3	90.8	85.3	88.4	90.2
S. hookeri	B (*Physolychnis*)	92.4	92.2	88.8	92.4	90.9	87.0	89.8	91.4
S. integripetala	B (*Sedoides*)	89.3	88.8	90.1	91.1	90.8	88.6	89.4	90.8
S. jeniseensis	S *(Siphonomorpha)*	92.4	92.9	87.8	94.0	91.4	85.3	88.7	91.7
S. koreana	S *(Siphonomorpha)*	92.9	93.4	88.8	92.7	91.3	84.7	90.1	91.6
S. laciniata	B (*Physolychnis*)	90.2	89.8	89.0	91.5	90.4	86.0	87.7	89.7
S. magellanica	B (*Physolychnis*)	88.5	87.5	87.7	88.9	89.6	86.8	88.7	88.8
S. marizii	B (*Melandrium*)	93.6	93.4	88.3	93.1	92.1	85.7	89.6	90.8
S. multiflora	S *(Siphonomorpha)*	91.4	90.3	89.0	91.1	91.2	86.2	89.6	92.7
S. nana	B (*Saponarioides*)	91.3	90.5	89.7	93.0	92.5	87.0	89.7	89.1
S. paradoxa	S *(Siphonomorpha)*	92.5	91.0	88.3	92.0	91.8	85.4	90.8	91.8
S. perlmanii	S (*Sclerophyllae*)	90.1	89.7	89.0	92.6	90.6	86.4	88.7	88.6
S. petersonii	B (*Physolychnis*)	92.9	93.2	87.6	92.3	90.5	84.6	88.7	90.8
S. regia	B (*Physolychnis*)	92.1	91.5	88.0	93.3	90.7	86.4	88.6	89.1
S. roemeri	S *(Siphonomorpha)*	87.9	87.5	91.5	92.2	92.1	91.0	89.1	86.7
S. samojedorum	B (*Physolychnis*)	92.2	91.3	89.8	94.2	92.0	86.6	89.5	90.2
S. saxatilis	S *(Siphonomorpha)*	89.9	89.8	89.0	91.1	90.5	87.8	89.4	92.0
S. spinescens	S *(Siphonomorpha)*	88.3	87.5	88.8	89.9	89.3	86.6	86.9	86.5
S. squamigera subsp. *vesiculifera*	S (*Lasiocalycinae*)	90.0	89.4	91.5	93.4	93.6	88.8	90.3	88.8
S. suksdorfii	B (*Physolychnis*)	87.4	86.5	88.5	91.5	87.8	88.6	85.2	86.5
S. swertiifolia	S (*Sclerocalycinae*)	91.4	91.5	86.5	89.7	89.6	82.3	91.0	93.6
S. vallesia* subsp. *vallesia	S (*Auriculatae*)	89.7	88.9	90.9	92.2	91.6	88.9	89.4	89.4
S. villosa	S *(Silene)*	92.7	91.4	83.8	87.6	88.9	81.1	91.1	93.3
S. virginica	B (*Physolychnis*)	90.8	91.7	86.4	91.8	88.9	84.7	86.6	88.1
S. viridiflora	S *(Siphonomorpha)*	92.5	92.6	89.3	92.3	92.2	85.6	90.7	91.0
S. waldsteinii	S *(Siphonomorpha)*	88.3	88.9	84.9	87.6	87.0	82.8	88.9	90.6
S. yunnanensis	B (*Cucubaloides*)	92.6	90.6	89.3	93.0	92.0	85.3	89.4	90.5

Table A3. Values of *J* index for the average silhouettes of each species with the eight lateral models: species giving higher values in model LM5 than in other models. In bold: species that did not reach the threshold value of 89.0 for the *J* index estimated as the mean of 20 seeds. B: corresponds to S. subg. *Behenantha*; S: corresponds to S. subg. *Silene*.

Species	Subgenus (Section)	LM1	LM2	LM3	LM4	LM5	LM6	LM7	LM8
S. caryophylloides	S (*Auriculatae*)	90.2	91.3	86.8	88.8	92.0	83.7	92.4	91.8
S. damascena	S *(Silene)*	89.8	89.5	91.1	90.3	93.9	87.6	91.7	88.1
S. legionensis	S *(Silene)*	88.4	87.0	90.3	88.9	91.1	88.5	88.5	86.8
S. linicola	S (*Lasiocalycinae*)	90.1	88.7	90.1	91.0	92.9	88.3	90.0	88.3
S. longicilia	S *(Siphonomorpha)*	90.6	90.1	91.7	92.1	93.6	88.4	91.0	90.1
S. multicaulis* subsp. *multicaulis	S *(Siphonomorpha)*	91.8	90.4	90.7	91.5	93.5	87.2	92.4	91.1
S. pomelii* subsp. *adusta	S *(Silene)*	90.1	89.4	85.6	86.8	90.2	80.3	89.6	88.1
S. pygmaea	S (*Auriculatae*)	91.3	89.8	90.7	92.4	92.8	87.7	91.0	90.7

Table A4. Values of *J* index for the average silhouettes of each species with seven dorsal models: species reaching maximum in convex models DM1, DM2, DM3, or DM4. In bold: species that did not reach the threshold value of 89.0 for the *J* index estimated as the mean of 20 seeds. B: corresponds to *S*. subg. *Behenantha*; S: corresponds to *S*. subg. *Silene*.

Species	Subgenus (Section)	DM1	DM2	DM3	DM4	DM5	DM6	DM8	DM9
S. aprica	B (*Physolychnis*)	91.3	91.8	90.1	91.3	91.1	91.2	82.4	66.7
S. baccifera	B (*Cuccubalus*)	87.2	88.1	90.3	90.3	81.2	89.2	86.6	68.1
S. fruticosa	S *(Siphonomorpha)*	92.2	93.3	94.3	92.6	89.8	86.7	81.2	64.7
S. hookeri	B(*Physolychnis*)	92.1	93.5	91.3	91.8	92.4	86.4	76.8	64.3
S. jeniseensis	S *(Siphonomorpha)*	93.0	92.5	90.7	90.6	89.7	89.5	83.9	67.5
S. koreana	S *(Siphonomorpha)*	89.9	88.9	89.7	90.6	86.6	90.6	87.4	69.1
S. marizii	B *(Melandrium)*	90.6	93.0	91.9	91.9	88.9	85.7	77.2	64.0
S. perlmanii	S(*Sclerophyllae*)	88.4	91.0	88.2	87.2	86.0	81.5	72.5	61.3
S. petersonii	B (*Physolychnis*)	91.7	93.7	93.5	93.4	90.2	87.6	80.4	65.7
S. virginica	B(*Physolychnis*)	92.9	92.9	92.0	91.8	90.0	89.3	85.1	68.0

Table A5. Values of *J* index for the average silhouettes of each species with seven dorsal models. Species reaching maximum in models DM5 or DM6. In bold: species that did not reach the threshold value of 89.0 for the *J* index estimated as the mean of 20 seeds. B: corresponds to *S*. subg. *Behenantha*; S: corresponds to *S*. subg. *Silene*.

Species	Subgenus (Section)	DM1	DM2	DM3	DM4	DM5	DM6	DM8	DM9
S. chlorifolia	S (*Sclerocalycinae*)	89.3	90.2	86.3	88.4	93.0	90.0	78.9	66.1
S. chungtienensis	B (*Physolychnis*)	89.2	88.8	87.5	89.4	88.9	92.3	82.8	68.5
S. chlorantha	S *(Siphonomorpha)*	78.5	78.1	78.6	80.9	79.3	87.2	85.6	78.2
S. damascena	S *(Silene)*	77.4	76.3	75.6	77.8	78.9	85.3	81.6	77.4
S. dichotoma	B *(Dichotomae)*	90.0	89.3	88.6	90.5	89.7	92.8	84.9	68.6
S. fabaria	B *(Behenantha)*	88.5	87.8	87.5	89.3	88.3	92.9	85.3	69.5
S. firma	B (*Physolychnis*)	89.3	88.9	89.1	90.9	88.5	91.9	88.0	70.5
S. foliosa	S *(Siphonomorpha)*	81.3	80.3	81.0	82.6	81.5	90.2	86.8	77.6
S. hayekiana	S *(Siphonomorpha)*	84.7	85.0	82.5	85.1	87.5	91.1	79.6	69.7
S. holzmannii	B *(Behenantha)*	87.0	90.1	86.1	89.5	91.3	85.0	73.0	63.4
S. integripetala	B (*Sedoides*)	81.5	80.7	81.9	84.3	80.9	89.8	88.7	76.7
S. legionensis	S *(Silene)*	85.2	82.6	83.2	85.8	85.6	92.7	84.7	71.2
S. linicola	S *(Lasiocalycinae)*	84.0	85.3	78.4	84.2	88.0	79.5	67.7	59.0
S. longicilia	S *(Siphonomorpha)*	80.4	79.1	79.6	81.6	80.6	89.0	84.8	76.2
S. multicaulis* subsp. *multicaulis	S *(Siphonomorpha)*	85.7	84.0	83.1	84.2	86.1	91.6	84.3	74.0
S. multiflora	S *(Siphonomorpha)*	86.4	85.3	85.1	88.0	86.5	92.9	86.8	70.6
S. nana	B (*Saponarioides*)	87.6	87.3	88.2	90.2	87.8	92.8	87.7	70.4
S. paradoxa	S *(Siphonomorpha)*	80.5	79.5	80.0	82.9	81.6	89.3	85.4	77.2
S. pygmaea	S (*Auriculatae*)	82.8	81.2	81.3	83.3	82.6	89.6	87.2	77.0
S. saxatilis	S *(Siphonomorpha)*	89.0	88.8	86.9	88.9	91.2	90.3	79.0	66.5
S. squamigera subsp. *vesiculifera*	S *(Lasiocalycinae)*	87.6	87.0	85.3	88.5	90.0	93.8	82.4	70.6
S. suksdorfii	B (*Physolychnis*)	89.6	88.8	90.2	90.1	87.2	91.1	88.5	70.1
S. villosa	S *(Silene)*	91.1	91.2	87.6	87.9	93.7	87.2	77.5	66.2
S. viridiflora	S *(Siphonomorpha)*	89.4	88.0	88.1	89.1	89.1	92.8	84.8	69.2

Table A6. Values of the *J* index for the average silhouettes of each species with seven dorsal models. Species reaching maximum in models DM8 or DM9. In bold: species that did not reach the threshold value of 89.0 for the *J* index estimated as the mean of 20 seeds. B: corresponds to S. subg. *Behenantha*; S: corresponds to S. subg. *Silene*.

Specie	Subgenus (Section)	DM1	DM2	DM3	DM4	DM5	DM6	DM8	DM9
S. bupleuroides	S (*Sclerocalycinae*)	66.7	65.8	68.1	67.8	63.2	71.9	79.0	86.3
S. caryophylloides	S (*Auriculatae*)	79.5	78.1	80.0	81.2	77.4	86.3	88.6	79.5
S. ciliata	S *(Silene)*	72.6	71.4	72.5	73.6	72.0	80.2	81.0	86.2
S. dinarica	S *(Siphonomorpha)*	77.5	76.6	78.9	78.0	73.9	82.1	88.8	77.2
S. frivaldskyana	S *(Siphonomorpha)*	76.9	75.7	77.0	78.5	76.5	84.8	85.2	82.6
S. gigantea	S *(Siphonomorpha)*	70.5	69.5	71.2	71.7	68.4	76.6	81.3	79.4
S. laciniata	B (*Physolychnis*)	64.0	65.9	69.0	67.4	58.6	67.5	79.2	80.2
S. magellanica	B (*Physolychnis*)	60.5	63.8	67.3	66.6	58.8	64.9	76.9	79.6
S. pomelii.* subsp. *adusta	S *(Silene)*	65.7	64.9	67.6	67.4	63.7	71.1	77.9	85.3
S. regia	B (*Physolychnis*)	81.4	80.0	81.9	82.0	79.3	85.7	89.0	76.0
S. roemeri	S *(Siphonomorpha)*	79.0	77.7	78.7	80.0	78.0	86.0	86.8	81.8
S. samojedorum	B (*Physolychnis*)	79.2	78.1	79.4	80.1	78.0	84.9	87.4	78.9
S. spinescens	S *(Siphonomorpha)*	74.0	73.1	74.6	76.0	72.6	80.4	85.7	85.4
S. swertiifolia	S (*Sclerocalycinae*)	67.8	66.7	69.0	68.8	65.2	72.8	80.2	86.0
S. vallesia* subsp. *vallesia	S (*Auriculatae*)	77.9	76.8	78.3	79.9	77.3	85.0	87.0	79.8
S. waldsteinii	S *(Siphonomorpha)*	72.1	70.5	72.6	73.8	71.2	78.8	82.9	88.3
S. yunnanensis	B (*Cucubaloides)*	80.8	79.2	80.3	81.9	79.6	86.8	87.1	77.1

Table A7. Data used in the construction of the dendrogram in Figure 21. In column 2, subg., B stands for *Behenantha*; S for *Silene*.

Species	Subg.	Section	LM2/4	LM5
S. aprica	B	*Physolychnis*	90.9	90.0
S. baccifera	B	*Cuccubalus*	93.2	88.1
S. chlorantha	S	*Siphonomorpha*	91.2	92.5
S. chlorifolia	S	*Sclerocalycinae*	91.6	90.9
S. chungtienensis	B	*Physolychnis*	91.7	89.9
S. damascena	S	*Silene*	90.1	92.8
S. dichotoma	B	*Dichotomae*	88.8	88.6
S. fabaria	B	*Behenantha*	90.0	89.4
S. firma	B	*Physolychnis*	92.3	88.8
S. fruticosa	S	*Siphonomorpha*	92.2	88.5
S. hookeri	B	*Physolychnis*	92.0	89.3
S. integripetala	B	*Sedoides*	89.1	87.8
S. jeniseensis	S	*Siphonomorpha*	91.8	88.3
S. koreana	S	*Siphonomorpha*	93.0	89.2
S. linicola	S	*Lasiocalycinae*	90.5	91.2
S. longicilia	S	*Siphonomorpha*	91.0	91.5
S. marizii	B	*Melandrium*	93.1	89.6
S. multiflora	S	*Siphonomorpha*	89.3	89.1
S. nana	B	*Saponarioides*	92.8	91.2
S. petersonii	B	*Physolychnis*	92.1	88.3
S. pygmaea	S	*Lasiocalycinae*	90.3	91.5
S. squamigera ssp. *vesiculifera*	S	*Lasiocalycinae*	90.3	92.7
S. suksdorfii	B	*Physolychnis*	91.1	87.8
S. villosa	S	*Silene*	91.4	91.5
S. virginica	B	*Physolychnis*	91.5	87.6
S. viridiflora	S	*Siphonomorpha*	91.9	89.8
S. yunannensis	B	*Cuccubaloides*	90.8	88.4

References

1. Boissier, E. *Flora Orientalis*; Georg, H. Basel: Geneva, Switzerland, 1867; Volume 1, pp. 567–656. Available online: https://www.biodiversitylibrary.org/item/60323#page/7/mode/1up (accessed on 2 February 2023).
2. Rohrbach, P. *Monographic der Gattung Silene*; Verlag von Engelmann: Leipzig, Germany, 1869; pp. 1–249. Available online: https://www.biodiversitylibrary.org/bibliography/15462 (accessed on 2 February 2023).
3. Chowdhuri, P.K. Studies in the genus *Silene*. *Notes Royal Bot. Gard. Edinburgh* **1957**, *22*, 221–287.
4. Ghazanfar, S.A. Seed characters as diagnostic in the perennial sections of the genus *Silene* L. (Family Caryophyllaceae). *Pakistan J. Bot.* **1983**, *15*, 7–12.
5. Fawzi, N.; Fawzy, A.; Mohamed, A. Seed morphological studies on some species of *Silene* L. (Caryophyllaceae). *Int. J. Bot.* **2010**, *6*, 287–292.
6. Bojňanský, V.; Fargašová, A. *Atlas of Seeds and Fruits of Central and East-European Flora: The Carpathian Mountains Region*; Springer: Berlin/Heidelberg, Germany, 2007; pp. 1–954.
7. Hoseini, E.; Assadi, M.; Edalatiyan, M.N.; Ghahremaninejad, F. Seed micromorphology and its implication in subgeneric classification of *Silene* (Caryophyllaceae, Sileneae). *Flora* **2017**, *228*, 31–38.
8. Atazadeh, N.; Keshavarzi, M.; Sheidai, M.; Gholipour, A. Seed morphology of *Silene commelinifolia* Boiss. complex (Caryophyllaceae Juss.). *Mod. Phytomorphol.* **2017**, *11*, 5–13.
9. Yildiz, K.; Cirpici, A. Seed morphological studies of *Silene* L. from Turkey. *Pak. J. Bot.* **1998**, *30*, 173–178.
10. Ullah, F.; Papini, A.; Shah, S.N.; Zaman, W.; Sohail, A.; Iqbal, M. Seed micromorphology and its taxonomic evidence in subfamily Alsinoideae (Caryophyllaceae). *Microsc. Res. Techniq.* **2019**, *82*, 250–259. [CrossRef]
11. Murru, V.; Grillo, O.; Santo, A.; Ucchesu, M.; Piazza, C.; Gaio, A.; Carta, A.; Bacchetta, G. Seed morpho-colorimetric analysis on some Tyrrhenian species of the *Silene mollissima* aggregate (Caryophyllaceae). *Flora* **2019**, *258*, 151445. [CrossRef]
12. Martín-Gómez, J.J.; Rodríguez-Lorenzo, J.L.; Juan, A.; Tocino, Á.; Janousek, B.; Cervantes, E. Seed Morphological Properties Related to Taxonomy in *Silene* L. Species. *Taxonomy* **2022**, *2*, 298–323. [CrossRef]
13. Martín-Gómez, J.J.; Rodríguez-Lorenzo, J.L.; Tocino, Á.; Janousek, B.; Juan, A.; Cervantes, E. The outline of seed silhouettes: A morphological approach to *Silene* (Caryophyllaceae). *Plants* **2022**, *11*, 3383. [CrossRef]
14. Martín-Gómez, J.J.; Rewicz, A.; Rodriguez-Lorenzo, J.L.; Janousek, B.; Cervantes, E. Seed morphology in *Silene* based on geometric models. *Plants* **2020**, *9*, 1787. [CrossRef]
15. Juan, A.; Martín-Gómez, J.J.; Rodriguez-Lorenzo, J.L.; Janousek, B.; Cervantes, E. New techniques for seed shape description in *Silene* species. *Taxonomy* **2022**, *2*, 1–19. [CrossRef]
16. Rodríguez-Lorenzo, J.L.; Martín-Gómez, J.J.; Tocino, Á.; Juan, A.; Janoušek, B.; Cervantes, E. New Geometric Models for Shape Quantification of the Dorsal View in Seeds of *Silene* Species. *Plants* **2022**, *11*, 958. [CrossRef] [PubMed]
17. Martín-Gómez, J.J.; Porceddu, M.; Bacchetta, G.; Cervantes, E. Seed Morphology in Species from the *Silene mollissima* Aggregate (Caryophyllaceae) by Comparison with Geometric Models. *Plants* **2022**, *11*, 901. [CrossRef] [PubMed]
18. Cervantes, E.; Rodríguez-Lorenzo, J.L.; Gutiérrez del Pozo, D.; Martín-Gómez, J.J.; Janousek, B.; Tocino, Á.; Juan, A. Seed Silhouettes as Geometric Objects: New Applications of Elliptic Fourier Transform to Seed Morphology. *Horticulturae* **2022**, *8*, 974. [CrossRef]
19. POWO. Plants of the World Online. Facilitated by the Royal Botanic Gardens, Kew. 2022. Available online: https://www.plantsoftheworldonline.org/ (accessed on 15 June 2022).
20. Jafari, F.; Zarre, S.; Gholipour, A.; Eggens, F.; Rabler, R.K.; Oxelman, B. A new taxonomic backbone for the infrageneric classification of the species-rich genus *Silene* (Caryophyllaceae). *Taxon* **2020**, *69*, 337–368.
21. Cervantes, E.; Martín-Gómez, J.J.; Espinosa-Roldán, F.E.; Muñoz-Organero, G.; Tocino, Á.; Cabello-Sáenz de Santamaría, F. Seed Morphology in Key Spanish Grapevine Cultivars. *Agronomy* **2021**, *11*, 734. [CrossRef]
22. Justice, O.L.; Bass, L.N. *Principles and Practices of Seed Storage, Agriculture Handbook, No. 506*; U.S. Department of Agriculture: Washington, DC, USA, 1978.
23. Shamrov, I.I. Diversity and typification of ovules in flowering plants. *Wulfenia* **2018**, *25*, 81–109.
24. Edalatiyan, M.N.; Joharchi, M.R.; Ghahremaninejad, F. *Silene ferdowsii* (Caryophyllaceae), a new species from Iran. *Ann. Bot. Fenn.* **2011**, *48*, 155–158. [CrossRef]
25. Ciocarlan, V.; Milanovic, S. *Silene thessalonica* discovered as part of the Romanian flora. *Acta Horti Bot. Bucurest.* **2009**, *36*, 61–62.
26. Gholipour, A. *Silene aminiradii* (Caryophyllaceae), an Interesting Alpine Plant in Iran. *Novon A J. Bot. Nomencl.* **2021**, *29*, 195–199. [CrossRef]
27. Lazkov, G.A.; Sennikov, A.N. Taxonomic assessment of three species of *Silene* (Caryophyllaceae) described by Boris K. Schischkin from Turkey. *Ann. Bot. Fennici* **2021**, *58*, 211–218. [CrossRef]

28. Bahmani, F.; Assadi, M.; Yildiz, K.; Mehregan, I. Phylogenetic relationships of *Silene* sections *Lasiostemones* and *Sclerocalycine* (Caryophyllaceae) in Iran. *Phytotaxa* **2020**, *441*, 274–284. [CrossRef]
29. Safaeishakib, M.; Assadi, M.; Mehregan, I.; Ghazanfar, S.A. Phylogenetic study of *Silene* sections *Auriculatae*, *Spergulifoliae*, *Ampullatae*, and *Lasiocalycinae* in Iran. *Phytotaxa* **2020**, *472*, 169–183. [CrossRef]